한국마린엔지니어링학회지 제32권, 제1호, pp. 82~93, 2008. 1 (ISSN 1226-9549)
Journal of the Korean Society of Marine Engineering

Numerical Investigation of Flow-pattern and Flow-induced Noise for Two Staggered Circular Cylinders in Cross-flow by LBM

Jeong-Whan Kim* · Sae-Kyung Oh** · Ho-Keun Kang†
(Manuscript : Received June 26, 2007 ; Revised Auquest 22, 2007)

Abstract : The flowfield behind two cylinders and flow-induced noise generated from the cylinders in various arrangement are numerically investigated based on the finite difference lattice Boltzmann model with 21 velocity bits, which is introduced a flexible specific heat γ to simulate diatomic gases like air. In an isolated cylinder with two type of mesh, some flow parameters such as Strouhal number S_t and acoustic pressure $\triangle p$ simulated from the solution are given and quantitatively compared with those provided the previous works. The effects of the center-to-center pitch ratio $L_{cc}/d=2.0$ in staggered circular cylinders as shown in Fig. 1 and angles of incidence $\alpha=30°(T_{cc}/d=0.5)$, $45°(T_{cc}/d=0.707)$ and $60°$ $(T_{cc}/d=0.866)$, respectively, are studied. Our analysis focuses on the small-scale instabilities of vortex shedding, which occurs in staggered arrangement. With the results of drag C_d and lift C_l coefficients and vorticity contours, the mechanisms of the interference phenomenon and its interaction with the two-dimensional vortical structures are present in the flowfields under Re $\leq$ 200. The results show that we successively capture very small pressure fluctuations, with the same frequency of vortex shedding, much smaller than the whole pressure fluctuation around pairs of circular cylinders. The upstream cylinder behaves like an isolated single cylinder, while the downstream one experiences wake-induced flutter. It is expected that, therefore, the relative position of the downstream cylinder has significant effects on the flow-induce noise, hydrodynamic force and vortex shedding characteristics of the cylinders.

Key words : Lattice Boltzmann method, Flow-induced noise, Staggered circular cylinders, Vortex shedding

1. Introduction

The flowfield and flow-induced noise around pairs of circular cylinders have been the subject of many studies in many forms and in different applications, both in nature and technology. Cylinder-like structures can be seen, both alone and in group, for examples in the designs for heat exchangers, cooling systems for nuclear power plants, under-structure of offshore

† Corresponding Author(Korean Register of Shipping), E-mail: kanghokeun@chol.com, Tel: 042-869-9215
* Korea Marine Equipment Research Institute
** School of Mechanical and Aerospace Engineering, Gyeongsang National University

platforms, buildings, chimneys, and struts, etc., in both air and water flow. In many of these cases, vortex shedding may be responsible for flow-induced noise and vibrations. The most general configuration of dual cylinders, of equal diameter, d, immersed in a steady mean cross-flow of velocity, U_∞, is known as the staggered arrangement as shown in Fig. 1. Here, the cylinders are spaced at a center-to-center distance, L_{cc}, and at an angle incidence, α, to the oncoming mean flow.

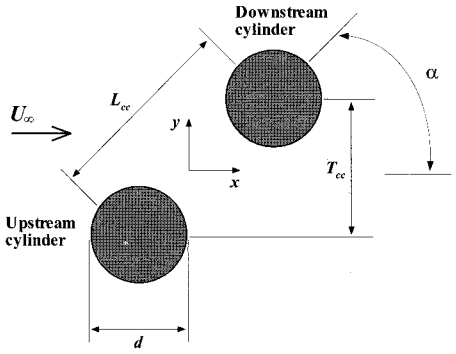

Fig. 1 Staggered arrangement of two circular cylinders of equal diameter in steady cross-flow

The complexity of the flow around the staggered arrangements has been reported in a number of experimental studies by Gu & Sun(1999)[1], Sumner et al.(2000)[2], Akosile & Sumner(2003)[3], and numerical ones by Johnson et al.(1993)[4], Mittal & Kumar(2001)[5], and Mittal & Raghuvanshi(2001)[6].

Gu and Sun(1999) was conducted the study at very high subcritical Reynolds numbers, which identified three main flow patterns for the staggered configuration. They presented that the complexity lies in the interaction of four separated free-shear layers, two Karman vortex formation and shedding process, and interactions between the two Karman vortex street. A similar studies for flow visualization and PIV experiments by Sumner et al.(2000) and Akosile & Sumner(2003) were conducted within the low subcritical regime Re=850~1900 have identified up to nine distinct flow patterns. These patterns incorporate various aspects of shear layer reattachment, alternate vortex shedding from one or both cylinders, vortex splitting, pairing and enveloping, synchronized vortex shedding, and vortex impingement.

Numerical computation of flows past periodic arrays of staggered cylinders consisting of either two or 10 cylinders was reported by Johnson et al.(1993). They established that the steady flows by dropping the time-derivative terms from the governing equations result in a significantly different solution compared with the time-averaged temporally periodic unsteady solutions. Moreover, an effort to explain the mechanism of control of vortex shedding with two circular cylinder of same diameter Mittal and Kumar (2001) and different ones by Mittal and Raghuvanshi (2001) at close proximity, the streamwise variation of the pressure coefficient close to the shear layer of the main cylinder was compared for various cases. They presented that the control cylinder provides a local favorable pressure gradient in the wake region, where the vortex shedding is suppressed, thereby stabilizing the shear layer locally. The numerical solution of flow-induced noise problems is still a major problem, which is often seen in various fields of

industry. Here, LBM seems to be the most promising method that computes directly source fluctuation in the flow for the prediction of flow noises, and at the same time the prediction of noise seems to be one of the most appropriate areas of engineering applications of LBM. Readers can refer to Kang et al.(2006; 2007)[7],[8] for a detailed description of the method. In the field of aerodynamic sounds some fundamental studies have been undertaken to show its validity concerning linear and nonlinear wave propagation by Buick et al. (2000)[9], acoustical streaming by Haydock and Yeomans (2001)[10], ultrasound gas flow meter by Wilde (2004)[11], and aeolian tone and edgetone by Kang and Tsutahara (2007)[8]. Buick et al.(2000) used the technique to simulate linear sound waves when the pressure variations are considered to be a small perturbation. They also extended the scope of the simulation to consider nonlinear waves and showed that the LBM and the incompressible approximation are not limited to the linear regime. Haydock and Yeoman(2001) reported to simulate the acoustical streaming produced by the interaction of an acoustic wave with a boundary. With comparison to Rayleigh streaming in appropriate limits, they showed how deviations from those limits affect the acoustic streaming. Wilde (2004) also investigated to the problem of a Helmholtz resonator under a grazing flow and to the propagation of sound waves in a turbulent flow in a duct of an ultra sound gas flow meter, showing great potential for the method in the field of flow acoustics. More recently, Kang and Tsutahara(2007) presented an novel approach to simulate aerodynamically generated sounds by modifying the finite difference-based lattice BGK model, demonstrating that their code is much cheaper with respect to the computational cost of the acoustic of DNS by Inoue and Hatakeyama (2002)[12]. So the use of the LBM as a tool for computational aerodynamic sounds can be seen in its early stage.

The present study by the finite difference-based lattice Boltzmann method (FDLBM), of a simple configuration of two circular cylinders of equal diameter arranged in a staggered configuration, in steady cross-flow, has been motivated by both fundamental and practical considerations. Moreover, it needs to further verify the numerical technique for multiple rigid cylinders in order to establish its credibility when applied to perform design analysis of multiple structures in a cross-flow.

This paper is organized as follows: the governing equations and numerical methods for the FDLBM with flexible specific heat ratio will be presented in Section 2. The accuracy of the code will be validated in Section 3 for some benchmark problems. Section 4 will be followed the flowfield behind two cylinder and flow-induced noise. In the final section, conclusions will be summarized.

2. Computational Methodology

2.1 Model of flexible specific heat ratio

As a newly developed numerical method, the LBM code, a novel kinetic-based

approach for simulating fluid flows and associated transport phenomena, has been successfully applied since it originated from the lattice gas cellular automata method (LGCA). Considered an attractive alternative to conventional finite difference schemes because it recovers the Navier-Stokes equations, the LBM is computationally more stable, and easily parallelizable.

However, most models in LBM are for incompressible fluids due to its simplicity of the structure, and only a few simulations by the models for compressible or thermal-fluid model have been reported by Alexander et al.(1993)[13], Chen et al.(1994)[14], and Tsutahara & Kang(2002)[15]. In the code, the mode of fluid particle is limited to that due to translation. The ratio of the specific heat γ, then, is $\gamma=(D+2)/D$ and D represents the space dimension. For the case of two-dimensional, the ratio of specific heats is $\gamma=2.0$, and it will apply to monatomic gases only but not to the diatomic gas such as air.

The modified model having energy modes except the translation $G_i(\mathrm{r},t)=f_i(\mathrm{r},t)E_i(\mathrm{r},t)$ to give the particle internal degree of freedom, which was originally proposed by Takada & Tsutahara(1999)[16] in LBM, is introduced in this code. The distribution function $G_i(\mathrm{r},t)$ is assumed to approach by collision to its local equilibrium state $G_i^{(0)}(\mathrm{r},t)$ as the particle distribution functions do, and the evolution of $G_i(\mathrm{r},t)$ is expressed as

$$\frac{\partial G_i}{\partial t}+c_{i\alpha}\frac{\partial G_i}{\partial x_\alpha}-\alpha c_{i\alpha}\frac{\partial}{\partial x_\alpha}\frac{G_i-G_i^{(0)}}{\phi}=-\frac{1}{\phi}\left(G_i-G_i^{(0)}\right) \quad (1)$$

Here, assumed that all the particles at the local equilibrium stage have the same rotational energy. Then the ratio of the specific heats γ is given as

$$\gamma=\frac{D+2}{D'}=\frac{D+D_E+2}{D+D_E} \quad (2)$$

where D' is the total degree of freedom of the particle motion and D_E is the degree of freedom of the rotation. The energy at the equilibrium stage E is expressed by

$$E=\frac{D}{2}\left(\frac{D+2}{D}-\gamma\right)e \quad (3)$$

$$G_i^{(0)}=Ef_i^{(0)} \quad (4)$$

When the flow is two-dimensional ($D=2$) and the degree of freedom of the rotation $D_E=1$, for example, the energy E will be $E=e/3$ and other energy $2e/3$ will be distributed to the translation modes, and then each energy is $e/3$. The energy, therefore, is equally distributed to each degree of freedom of motion, and γ can be freely variable as follows.

$$1.0<\gamma\le\frac{D+2}{D} \quad (5)$$

In Eq.(4), the local equilibrium distribution function for 21 velocity bits is given by

$$f_i^{(0)}\cong F_i\rho\left[1-2Bc_{i\alpha}u_\alpha+2B^2(c_{i\alpha}u_\alpha)^2+Bu_\alpha u_\beta-\frac{4}{3}B^3(c_{i\alpha}u_\alpha)^3-2B^2c_{i\alpha}u_\alpha u_\beta u_\gamma\right] \quad (6)$$

in which the subscript α represents Cartesian coordinates. The constants F_i and B are explained in Ref.[8].

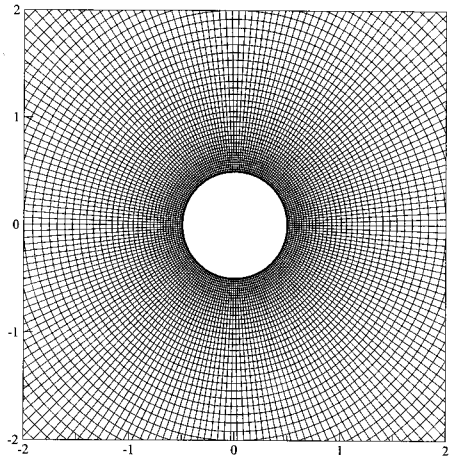

(a) O-grid mesh

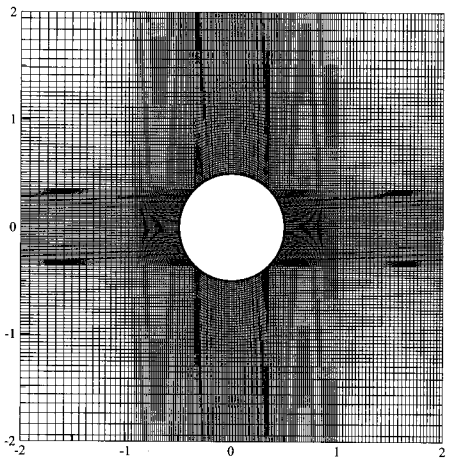

(b) H-grid mesh

Fig. 2 Two kinds of computational grid for circular cylinders (enlarged)

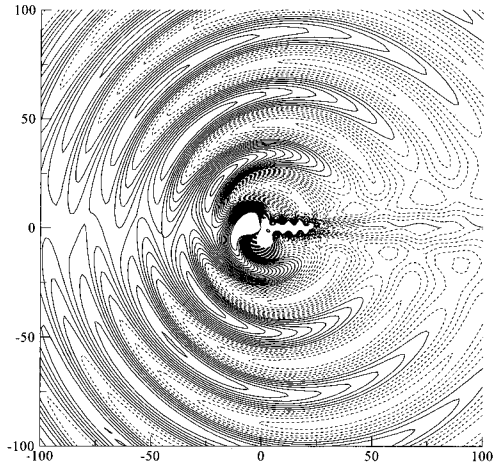

(a) O-grid mesh (T=135)

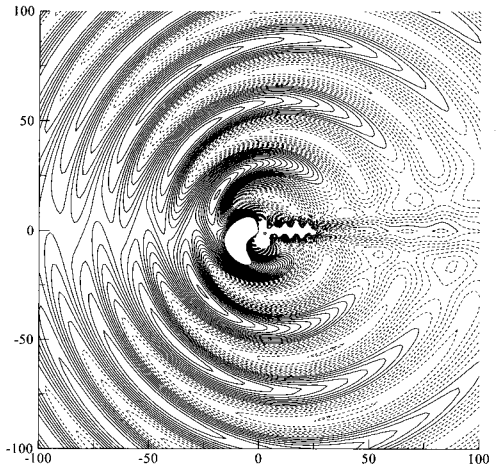

(b) H-grid mesh (T=182)

Fig. 3 Contours of sound pressure for two different mesh. The contour level fluctuates at $\triangle p_{step}=7\times10^{-4}$, respectively. M=0.2, Re=150.

3. Results and Discussion

3.1 Validation of the code

Flow past an isolated circular cylinder is a well- studied benchmark problem. The study of flow past an isolated circular cylinder can also be used to validate the present computational code. Moreover, to analyse and understand the vortex shedding behaviour and the interference of vortex streets behind the two circular cylinders, the solution of flow past an isolated circular cylinder can serve as a reference for comparison.

Two-dimensional flowfields in a Reynolds number range varying from 100 to 200 are carried out. The Reynolds number Re $= Ud/\nu$ is defined in terms of the cylinder diameter d, the free stream velocity U and the viscosity of the fluid.

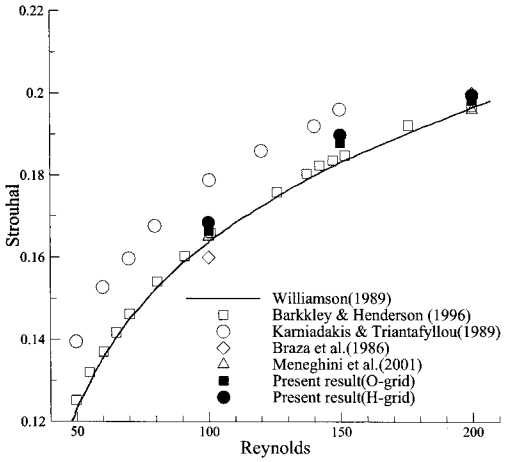

Fig. 4 Comparison of Strouhal number between experimental and numerical results[17]-[21]

First of all, to confirm the lattice dependence, we consider the flows and the noise generated by two kinds of mesh as shown in Fig. 2. The computational domain is extended to $-150d \le x \le 150d$ and $-150d \le y \le 150d$, where d is the cylinder diameter. The same minimum lattice length of $\Delta s_{\min}=0.001$ on the cylinder surface is given for both cases. The initial conditions are set to Re=100~200, $U_0=0.2$, $\gamma=1.4$ and internal energy $e_0=0.5$, respectively.

Fig. 3 illustrate the typical acoustic pressure contours at an instantaneous time. The solid lines indicate the positive pressures and the dashed lines are negative ones. As can be seen from these figures, rarefaction waves with negative Δp and compression waves with positive Δp are generated alternately around the cylinders at the origin, and it propagate downstream and upstream, respectively. Furthermore, these results verify that the acoustic waves have an isotropic characteristic regardless of the type of meshes.

The results for Reynolds number varying from about 50 to 200 are summarized and compared to other calculations and experiments in Fig. 4. For these Re the Strouhal numbers obtained here are the almost same as the value obtained by other literature data for these Reynolds numbers, as can be seen in the figure. The agreement here is very good, showing the applicability of the present code to study vortex shedding and flow-induced noise from circular cylinders. Hereafter we just use the type of H-grid mesh.

3.2 Flowfield past staggered arrangement in two cylinders

3.2.1 Flow patterns

The staggered arrangement of cylinders is the one that is most likely to occur in an engineering situation, for example, in heat exchangers and other cooling systems involving tube bundles. As compared with the flowfields behind one isolated circular cylinder, the flowfields behind two circular cylinders are much more complicated, especially for the case where the intense flow dynamic activity is noticed in the gap region between the cylinders.

The flow patterns, shown schematically in Figs. 5 to 7, are identified from the vorticity images and force coefficients, depending on the geometrical parameters L_∞/d and T_∞/d. The flow patterns cover staggered configurations of $L_\infty/d=2.0$, and $\alpha=30°$ ($T_\infty/d=0.5$), 45° ($T_\infty/d=0.707$) and 60° ($T_\infty/d=0.866$) for large angles of incidence at Re=150 $U_0=0.2$ and $\gamma=1.4$. Reynolds number is based on the diameter

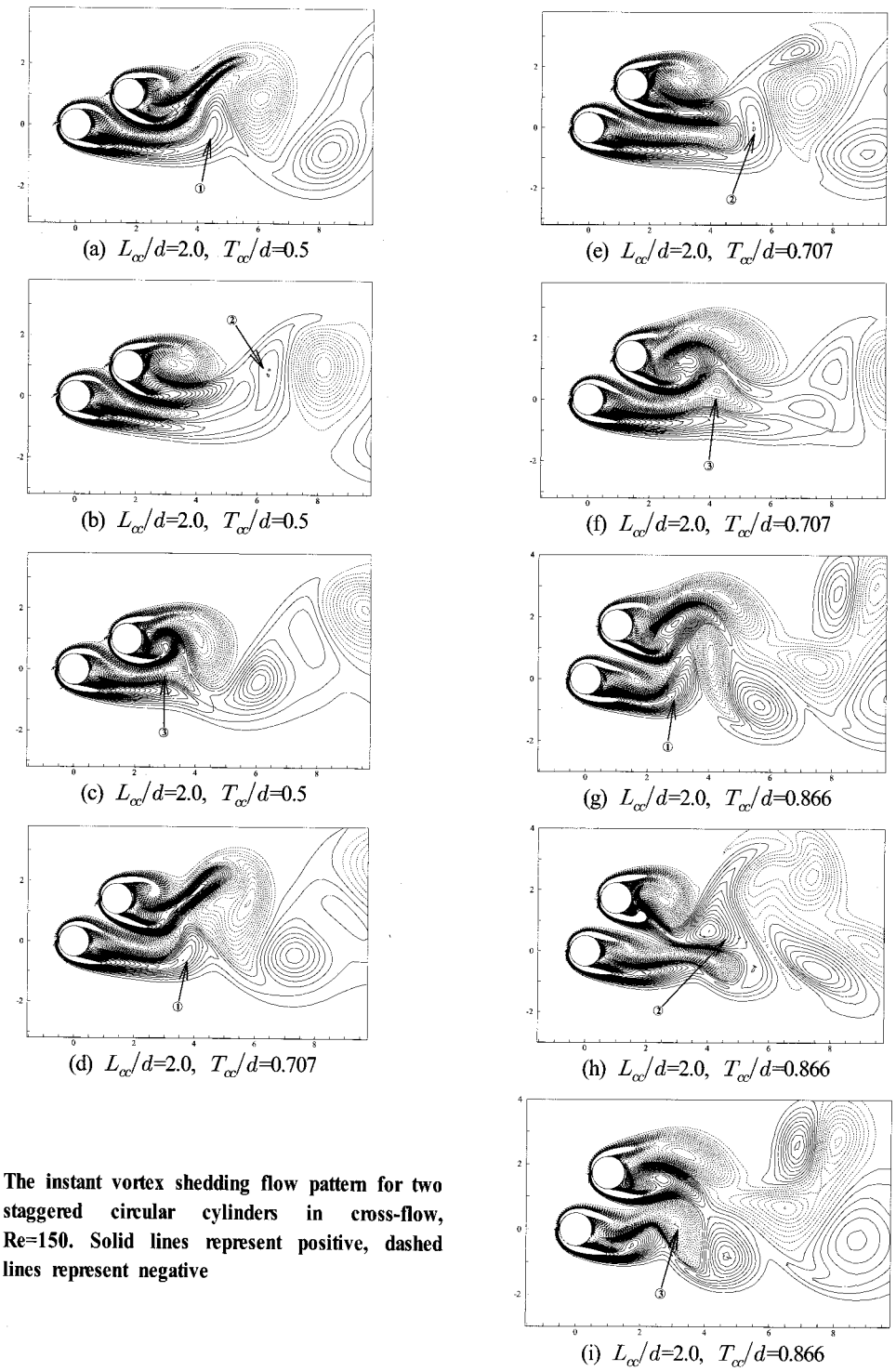

(a) L_{cc}/d=2.0, T_{cc}/d=0.5

(b) L_{cc}/d=2.0, T_{cc}/d=0.5

(c) L_{cc}/d=2.0, T_{cc}/d=0.5

(d) L_{cc}/d=2.0, T_{cc}/d=0.707

(e) L_{cc}/d=2.0, T_{cc}/d=0.707

(f) L_{cc}/d=2.0, T_{cc}/d=0.707

(g) L_{cc}/d=2.0, T_{cc}/d=0.866

(h) L_{cc}/d=2.0, T_{cc}/d=0.866

(i) L_{cc}/d=2.0, T_{cc}/d=0.866

Fig. 5 The instant vortex shedding flow pattern for two staggered circular cylinders in cross-flow, Re=150. Solid lines represent positive, dashed lines represent negative

of the cylinders, free-stream velocity and the viscosity of the fluid. The nondimensional distance between the gaps of the two cylinders is denoted by L_{α}/d in the flow direction and by T_{α}/d in the cross-flow direction as shown in Fig. 1. In the rest of the article we will refer to the upstream cylinder as cylinder 1 and to the downstream one as cylinder 2. The fluid domain is given to $-100d \le x_{cyl1} \le 102d$ and $-100d \le y_{cyl1} \le 102d$ and the minimum lattice length is set to $\Delta s_{\min} = 0.001$ on the two cylinder surfaces.

Fig. 5 show the process of vortex shedding from the cylinders in various arrangements. As shown in the figures, the counter-clockwise rotating vortices (see arrow ① of Figs. (a), (d), (g)) that are shed from the lower surface of the upstream cylinder pass the below the downstream cylinder and interact with (see arrow ② of Figs. (b), (e), (h)) the counterclockwise rotating vortices shed from its lower surface. The two coalesce downstream and one can observe a row of counterclockwise rotating vortices that are elongated along the flow direction. The clockwise rotating vortices ③ that are shed from the upper surface of the upstream cylinder hit the rear one and split into two. The one that glides along the lower surface gets diffused quite soon, while the one that moves towards the upper surface of the downstream cylinder interacts with its clockwise rotating vortex. Consequently, this interaction produces a stronger vortex that is shed from the upper surface of the downstream that a row of such vortices is observed in the wake. Within the combined wake of the pair of cylinders, this results in two adjacent Karman vortex streets that exhibit anti-phase synchronization. The flow pattern is similar that for the side-by-side circular cylinder, at intermediate and moderately large L_{α}/d by Summer et al.(1999). Furthermore, Fig. 6 illustrates the flow pattern behind two circular cylinders (side-by-side configuration: $L_{\alpha}/d=2.0$), and also similar that of Summer et al.[10]. But in this paper we do not discuss the flowfields for the side-by-side configuration.

In the near-field flow structure, time evolutions of drag C_l and lift C_d forces acting on both cylinders are shown in Fig. 7. As shown in these figures, the drag and lift coefficients synchronize variation with time, which also confirm the synchronized behaviour of vortex shedding from the upstream and downstream cylinders. After the vortex shedding starts, the drag and lift coefficients for downstream cylinder more greatly fluctuate than that of the upstream cylinder. This is because the downstream cylinder has a greater influence on the wake of the upstream cylinder. In fact, the small instant fluctuations in the lift and drag for the upstream cylinder are due to the vortex shedding behind the downstream cylinder.

3.2.2 Flow-induced noises

Fig. 8 shows the time history of sound pressure at 2 points in calculating domain. The observation points are radically considered on the center of upstream cylinder(x_0, y_0), in which these points apart from $(7.5d, 37.5)$ in the x and y direction, respectively. The sound signals fluctuate with a period of $\Delta T(= Ut/d) = 8.077$, 7.5 and 6.774, which correspond to $S_t(= fd/U) =$ 0.124, 0.133 and 0.147, respectively.

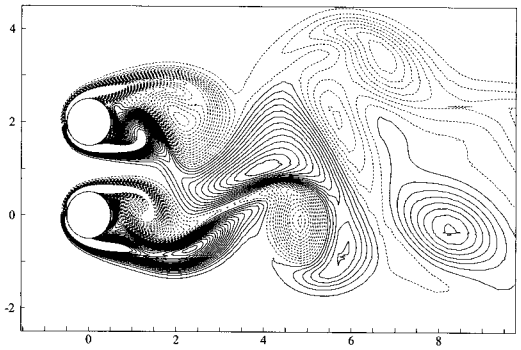

Fig. 6 Vorticity contours, side-by-side arrangement L_{cc}/d=2.0 (Re=200)

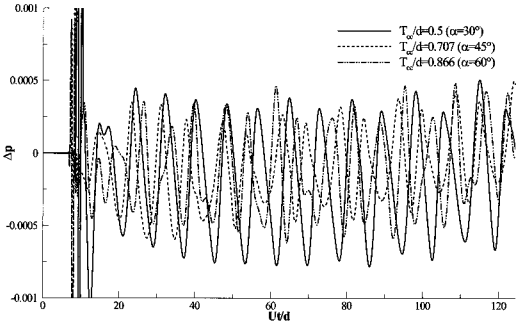

Fig. 8 Time variation of acoustic pressure for three different incident angles (L_{cc}/d=0.5. 0.707 and 0.866). The measured position is (7.5*d*, 37.5)

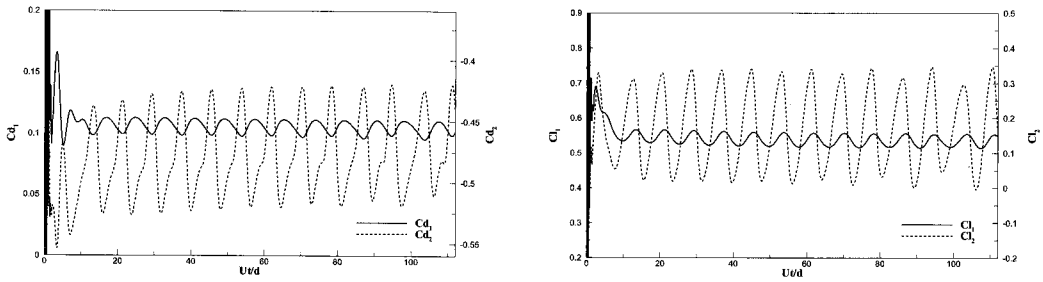

(a) L_{cc}/d=2.0, T_{cc}/d=0.5

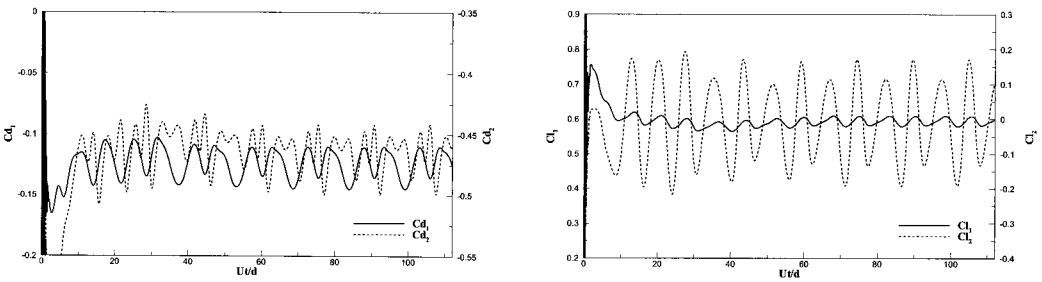

(b) L_{cc}/d=2.0, T_{cc}/d=0.707

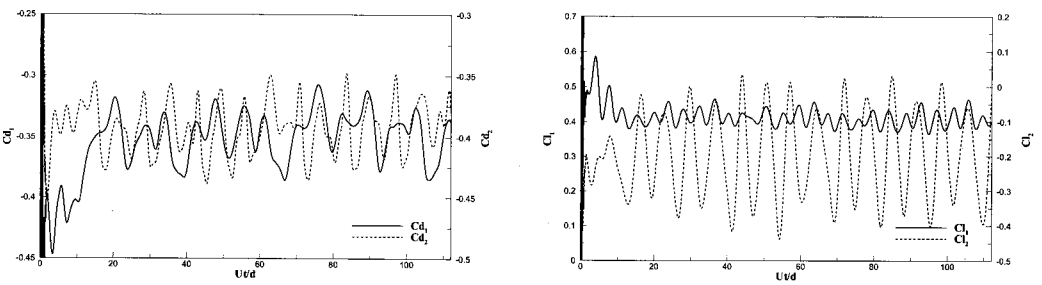

(c) L_{cc}/d=2.0, T_{cc}/d=0.866

Fig. 7 Drag and lift coefficients of flow past a pair of staggered cylinders at Re=150

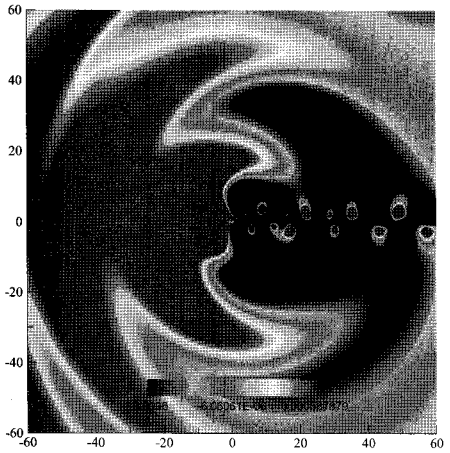

(a) L_{cc}/d=2.0, T_{cc}/d=0.5

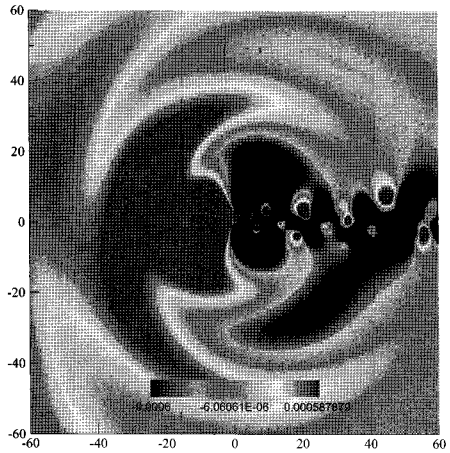

(b) L_{cc}/d=2.0, T_{cc}/d=0.707

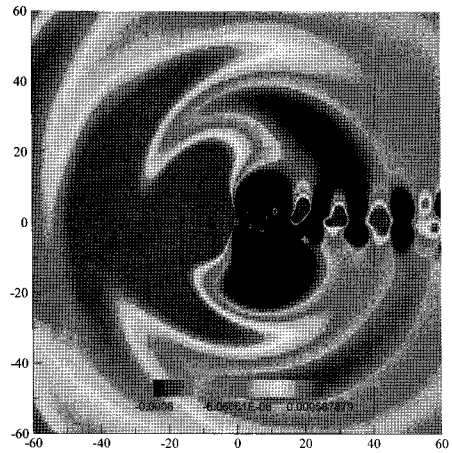

(c) L_{cc}/d=2.0, T_{cc}/d=0.866

Fig. 9 Acoustic pressure distribution (Δp_{step} =7×10^{-4})

Fig. 9 shows the acoustic pressure field at T=125 for three different incident angles (α=30°, 45° and 60°), where the contour level fluctuates at Δp_{step}=6.0×10^{-4}. The solid lines indicate the positive pressures and the dashed lines are the negative ones. As can be seen from this figure, rarefaction waves with negative Δp and compression waves with positive Δp are emitted alternately around the cylinders at the origin, and propagate upstream and downstream, respectively.

4. Conclusions

The use of a modified FDLB model of 2D 21 bits for simulating flow noise by dual cylinders is considered. A staggered configuration of two circular cylinders with equal diameter is examined under steady upstream cross-flow conditions for Re=150 and γ=1.4.

For the case of flows past two cylinders it is observed that the downstream cylinder, which lies in the wake of the upstream cylinder, experiences very large unsteady forces that can give rise to wake-induced flutter. Therefore, it is assumed that the relative position of the downstream cylinder has significant effect on the flow-induce noise, hydrodynamic forces and vortex shedding characteristics.

The successful simulation of the complex flow phenomenon for two staggered circular cylinders demonstrates the robustness and flexibility of the present code.

References

[1] Z. F. Gu and T. F. Sun, "On Interference between Two Circular Cylinders in Staggered Arrangement at High Subcritical Reynolds Numbers", J. Wind Eng. Indust. Aerodyn., Vol. 80, pp. 287-309, 1999.

[2] D. Sumner, S. J. Price and M. P. Paidoussis, "Flow-pattern Identification for Two Staggered Circular Cylinders in Cross-flow", J. Fluid Mech., Vol. 411, pp. 263-303, 2000.

[3] O. O. Akosile and D. Sumner, "Staggered Circular Cylinders Immersed in a Uniform Planar Shear Flow", J. Fluids Struct., Vol. 18, pp. 613-633, 2003.

[4] A. A. Johnson, T. E. Tezduyar and J. Liou, "Numerical Simulation of Flows Past Periodic Arrays of Cylinders", Comput. Mech., Vol. 11, pp. 371-383, 1993.

[5] S. Mittal and V. Kumar, "Flow-induced Oscillations of Two Cylinders in Tandem and Staggered Arrangements", J. Fluids Struct., Vol. 15, pp. 717-736, 2001.

[6] S. Mittal and A. Raghuvanshi, "Control of Vortex Shedding behind Circular Cylinder for Flows at Low Reynolds Numbers", Int. J. Numer. Meth. Fluids, Vol. 35, pp. 421-447, 2001.

[7] H. K. Kang, S. W. Ahn and J. W. Kim, "Application of Subgrid Turbulence Model to the Finite Difference Lattice Boltzmann Method", J. Kor. Soc. Marine Eng., Vol. 30, No. 5, pp. 580-588, 2006.

[8] H. K. Kang and M. Tsutahara, "An Application of the Finite Difference-based Lattice Boltzmann Model to Simulating Flow-induced Noise", Int. J. Numer. Meth. Fluids, Vol. 53, pp. 629-650, 2007.

[9] J. M. Buick, C. L. Buckley, C. A. Greated and J. Gilbert, "Lattice Boltzmann BGK Simulation of Nonlinear Sound Waves: the Development of a Shock Front", J. Physics A, Vol. 33, pp. 3917-3928, 2000.

[10] D. Haydock and J. Yeomans, "Lattice Boltzmann Simulations of Acoustic Streaming", J. Physics A, Vol. 34, pp. 5201-5213, 2001.

[11] A. Wilde, "Flow Acoustic Simulations Using the Lattice-Boltzmann Method", Int. Con. on FEM Tech. with ANSYS & ICEM CFD Conf., Germany, 2004.

[12] O. Inoue and N. Hatakeyama, "Sound Generation by a Two- dimensional Circular Cylinder in a Uniform Flow", J. Fluid Mech., Vol. 471, pp. 285-314, 2002.

[13] F. J. Alexander, S. Chen and D. J. Sterling, "Lattice Boltzmann Thermodynamics", Phys. Rev. E., Vol. 47, pp. 2249-2252, 1993.

[14] Y. Chen and G. D. Doolen, "Lattice Boltzmann Method for Fluid Flow", Ann. Rev. Fluid Mech., Vol. 30, pp. 329-364, 1998.

[15] M. Tsutahara and H. K. Kang, "A Discrete Effect of the Thermal Lattice BGK Model", J. Stat. Phys., Vol. 107, Nos.1/2, pp. 479-498, 2002.

[16] N. Takada and M. Tsutahara, "Proposal of Lattice BGK Model with

Internal Degrees of Freedom in Lattice Boltzmann Method", Trans. JSME J., B, Vol. 65, No.629, pp. 92-99, 1999.

[17] C. H. K. Williamson, "Oblique and Parallel Modes of Vortex Shedding in the Wake of a Circular Cylinder at Low Reynolds Numbers", J. Fluid Mech., Vol.206, pp. 579-627, 1989.

[18] D. Barkley and R. D. Henderson, "Three-dimensional Floquet Stability Analysis of the Wake of a Circular Cylinder", J. Fluid Mech., Vol.332, pp. 214-241, 1997.

[19] G. E. Karniadakis and G. S. Triantafyllou, "Frequency Selection and Asymptotic States in Laminar Wakes", J. Fluid Mech., Vol.199, pp. 441-469, 1989.

[20] M. Braza, P. Chassaing and H. Ha Minh, "Numerical Study and Physical Analysis of the Pressure and Velocity Fields in the Near Wake of a Circular Cylinder", J. Fluid Mech., Vol.165, pp. 79-130, 1986.

[21] J. R. Meneghini and F. Saltara, "Numerical Simulation of Flow Interference between Two Circular Cylinders in Tandem and Side-by-side Arrangement", J. Fluids Struct., Vol.15, pp. 327-350, 2001.

Author Profile

Jeong-Whan Kim

He graduated from Pukyung National University (B.A. 1998 and M.S. 2000) in Korea. He received his Ph.D degree from Pukyung National University in Korea. He currently works at Korea Marine Equipment Research Institute.

Sae-Kyung Oh

He graduated from Pukyung National University (B.A. 1973 and M.S. 1988) in Korea. He received his Ph.D degree from Pukyung National University in Korea. He currently works at Gyeongsang National University for 32 years as a professor.

Ho-Keun Kang

He graduated from Korea Maritime University(B.A. 1992 and M.S. 1997) in Korea. He received his Ph.D degree (2002) from Kobe University in Japan. He worked at Gyeongsang National University for 6 years as a research professor. He currently works in Korean Register of Shipping (KR). His interests are CFD, fluid-induced noises by Lattice Boltzmann Method, and various energy problems including renewable energy.